The Effect of Arterial Cannula Tip Position on Differential Hypoxia During Venoarterial Extracorporeal Membrane Oxygenation

Avishka Wickramarachchi (avishka.wickramarachchi@monash.edu)
CREATElab, Monash University
Aidan J.C. Burrell
Alfred Hospital
Andrew F. Stephens
CREATElab, Monash University
Michael Šeman
CREATElab, Monash University
Ashkan Vatani
CREATElab, Monash University
Mehrdad Khamooshi
CREATElab, Monash University
Jaishankar Raman
University of Melbourne, Austin & St Vincent's Hospitals
Rinaldo Bellomo
Austin Hospital
Shaun D. Gregory
CREATElab, Monash University

Research Article

Keywords: cannula position, mixing zone, watershed region, harlequin syndrome, computational fluid dynamics.

Posted Date: April 11th, 2022

DOI: https://doi.org/10.21203/rs.3.rs-1535294/v1

Abstract

Background: The interaction between native left ventricular output and venoarterial extracorporeal membrane oxygenation (VA ECMO) flow may hinder perfusion of oxygenated blood to the aortic arch branches, resulting in differential hypoxia. Typically, the arterial cannula tip is placed in the iliac artery or abdominal aorta. However, the hemodynamics of an advanced arterial cannula tip have not been studied before. This simulation study aimed to investigate the effect of altering arterial cannula tip position on VA ECMO perfusion to the upper extremities.

Methods: Computational fluid dynamics simulations were performed using a patient-specific geometry of the aorta and physiologically representative boundary conditions. Four arterial cannula tip positions (P1. common iliac, P2. abdominal aorta, P3. descending aorta and P4. aortic arch) were compared with different degrees of cardiac dysfunction and VA ECMO support (50%, 80% and 90% VA ECMO support).

Results: P4 was able to supply oxygenated blood to the arch vessels at all support levels, while P1 to P3 only perfused the arch vessels with the highest level (90%) of VA ECMO support. Even during the highest level of support, P1 to P3 could only provide oxygenated VA ECMO flow at 0.11 L/min to the brachiocephalic artery, compared with 0.5 L/min at P4.

Conclusions: Advancing the arterial cannula tip into aortic arch increased the perfusion of blood from VA ECMO to the aortic arch vessels at all simulated support levels. In contrast, the tip position used in standard clinical practice was predicted to result in differential hypoxia during 50% and 80% support with only a slight improvement at 90% support. Therefore, during VA ECMO, advancing the arterial cannula tip has the potential to improve upper body perfusion and reduce the risk of differential hypoxia.

Background

Venoarterial extracorporeal membrane oxygenation (VA ECMO) is an established form of mechanical circulatory support for patients with refractory cardiac or cardio-pulmonary failure. In VA ECMO, the arterial return cannula is positioned in the arterial system and while multiple different arterial access sites can be used, the femoral artery is the most common having been demonstrated to have faster and easier access, with a lower risk of bleeding complications [1–3]. When cannulating via the femoral artery, the cannula tip typically lies within the abdominal aorta or common iliac artery, with flow from the cannula traveling in a retrograde direction, against the forward flow produced by the heart. The junction of flow from the cannula and antegrade flow from the left ventricle forms a watershed region or mixing zone. The location of this region can impact VA ECMO perfusion of parts of the upper and lower body. Patients with impaired pulmonary function coupled with increasing cardiac output can lead to a state whereby proximal aortic branch vessels are perfused with blood of lower oxygenation saturation. In contrast, distal to the mixing zone, tissues and organs are perfused by oxygenated VA ECMO flow. This phenomenon is known as differential hypoxia. It can result in cerebral and coronary hypoxia, and is associated with

increased rates of adverse clinical outcomes, including neurological complications and reduced survival [4–6].

In recent years, computational fluid dynamics (CFD) have been increasingly used as research tools to obtain insights in how to optimize mechanical circulatory support strategies. CFD enables researchers to investigate the effect of different cannula positions on pressure and flow fields, including mixing zones, with spatial and temporal resolution unattainable by clinical methods. Previous studies have used CFD to investigate the effect of increasing cannula flow rate on mitigating differential hypoxia [7–11]. Investigators concluded high ECMO flow rates (> 4.5 L/min) were required to mitigate differential hypoxia, and even then, small quantities of cardiac output were able to shift the mixing zone distally, thereby reducing flow rates of oxygenated blood to the upper body. Advancing the cannula tip to a more proximally located position has been suggested as a possible method to mitigate differential hypoxia, but the hemodynamics of such a solution has not been studied previously [12].

The aim of this study was to evaluate how altering cannula tip position impacts mixing zone location and flow field characteristics which might be conducive to differential hypoxia. For this purpose, a CFD simulation was constructed using patient specific geometry and physiologically representative boundary conditions. Cannula tip positions were varied in simulations of different degrees of cardiac dysfunction and VA ECMO support. We hypothesized that VA ECMO perfusion of the aortic arch branch vessels could be improved by positioning the cannula tip closer to the aortic arch.

Methods

Geometry

A 3D model of the aorta and its major branches was extracted from a computed tomography (CT) scan of the chest, abdomen and pelvis of a male patient undergoing VA ECMO. The patient had VA ECMO initiated in an extracorporeal cardiopulmonary resuscitation (ECPR) setting due to pulseless electrical activity arrest secondary to an ST-elevation myocardial infarction. The patient was 44 years of age, 175 cm in height and weighed 80 kg. Image segmentation was performed using MIMICS 21.0 and 3-Matic 21.0 image processing software (Materialise NV., Leuven, Belgium) where contrast thresholds were manipulated to obtain the blood volume of the aorta. The aortic branches extracted for this study included the brachiocephalic artery (BCA), left common carotid artery (LCCA), left subclavian artery (LSCA), coeliac axis/trunk, superior and inferior mesenteric arteries (SMA and IMA, respectively), left and right renal arteries and left and right common iliac arteries (LCI and RCI, respectively). The model was then imported into SpaceClaim (SpaceClaim Corporation, MA, USA) to perform 3D design modelling. Here, a 19 Fr Maquet HLS (Getinge, Rastatt, Germany) arterial cannula tip was placed in the right common iliac artery (P1). Three other cannula tip positions, each progressively more proximal, were created to represent advancement of the arterial cannula towards the aortic arch: position 2 (P2) in the abdominal aorta; position 3 (P3) in the distal portion of the descending aorta; and position 4 (P4) in the distal section of the aortic arch (Fig. 1). Before performing CFD simulations, each geometry was meshed.

This involved reconstructing the entire anatomical domain with many finite elements. This was done so that the governing fluid equations could be solved within these elements to provide local approximations of the solution. The meshes used in this study contained between 0.6 and 1 million poly-hexcore elements and was meshed using Fluent 20R2 (ANSYS, Canonsburg, Pennsylvania, USA). All simulations were then performed using ANSYS Fluent. Further details regarding the meshing process for this study can be found in the supplementary material (Additional File 1).

Figure 1: Cannula tip positions investigated. Position 1, in the right iliac artery; Position 2, in the abdominal aorta; Position 3, in the descending aorta; and Position 4, in the aortic arch. BCA – brachiocephalic artery, LCCA – left common carotid artery, LSCA – left subclavian artery, L-Renal – left renal, R-Renal – right renal, SMA – superiormesenteric artery, IMA – inferiormesenteric artery, RCI – right common iliac, LCI – left common iliac.

Boundary Conditions and Model Set-up

Boundary conditions at the outlets of each arterial branch were created using a 3-element Windkessel model to incorporate the effects of the distal vasculature and the dynamic nature of the systemic circulation [13]. The 3-element Windkessel functions lump components of the systemic circulation into peripheral and distal resistances whilst also incorporating compliance effects. Further details regarding these boundary conditions are outlined in the supplementary material (Additional File 2).

The two inlets for this CFD model consisted of the cannula tip and the aortic valve. The cannula produced a constant flow whilst a pulsatile flow waveform was prescribed at the aortic valve inlet using patient derived measurements from the literature [14]. Total flow (aortic valve flow + VA ECMO flow) entering the system was kept constant at 5 L/min throughout all simulations as per previous studies [7, 8]. Native output and VA ECMO flow were then varied accordingly to reflect various degrees of cardiac dysfunction and VA ECMO support. The following scenarios were simulated: 50% support (2.5 L/min native flow and 2.5 L/min from VA ECMO), 80% support (1 L/min native flow and 4 L/min from VA ECMO), and 90% support (0.5 L/min native flow and 4.5 L/min from VA ECMO). A baseline healthy scenario (5 L/min native flow and 0 L/min from VA ECMO) without a cannula in-situ, was also simulated to serve as a control for vessel perfusion flow rates. The healthy transaortic valve flow waveform was scaled to produce the aforementioned degrees of failure (Fig. 2) [14].

All vessel walls were assumed to be rigid and a no-slip boundary condition was imposed. The non-Newtonian behavior of blood was modelled using the Carreau model to maintain physiological accuracy, accounting for pulsatility and shear thinning properties [15, 16]:

$$\eta = \eta_\infty + \left(\eta_0 + \eta_\infty\right)\left(1 + \gamma^2\lambda^2\right)^{\frac{n-1}{2}}$$

2

where η is the local viscosity, $\eta_\infty = 0.00345$ kg/(m.s), $\eta_0 = 0.056$ kg/(m.s), γ is the local shear rate, $\lambda = 3.313$ s, and n = 0.3568 [15].

The implicit formulation of the Volume of Fluid multiphase model was chosen to distinguish between blood from the left ventricle (LV) and the VA ECMO circuit. Turbulence was modelled using the k-ω Shear Stress Transport model and the Pressure-Implicit with Splitting of Operators algorithm was adopted for the pressure-velocity coupling method. The time step was set as 0.001 s and 15 cardiac cycles were simulated to ensure convergence was achieved. Additionally, the solution at each time step was considered converged when the scaled residuals value decreased below 10^{-4}. All simulations were performed on a high-performance cluster (Multi-modal Australian ScienceS Imaging and Visualisation Environment) at Monash University, Melbourne, Australia.

Figure 2: Scaled aortic valve inlet profiles to reflect different severities of cardiac dysfunction. Here, 100% reflects healthy cardiac function where 5 L/min of cardiac output from the left ventricle. 50%, 20% and 10% depicts cardiac failure where only 2.5, 1 and 0.5 L/min of cardiac output from the left ventricle, respectively.

Results

Results from each simulation were obtained quantitatively and qualitatively. The flow rates of blood received from VA ECMO perfusion at all aortic branches are presented in Fig. 3. Aortic branch vessel flow rates for a simulated healthy adult (without VA ECMO) is also shown in Fig. 3. Mixing zone locations for cannula tip positions according to increasing level of VA ECMO support are shown in Fig. 4. This data reflects mixing zone locations at end-diastole.

50% VA ECMO Support

During this scenario, P4 was the only position which perfused all aortic arch branch vessels with blood from VA ECMO. Total flow to these vessels were comparable in magnitude to healthy conditions as it contained blood from both the LV (deoxygenated) and blood from VA ECMO (oxygenated). However, the flow rates of blood from VA ECMO to the BCA, LCCA and LSCA were 0.29, 0.06 and 0.32 L/min, respectively (Fig. 3). Compared to a healthy adult, these flow rates reflect 54%, 55% and 76% of normal flow rates usually seen in the BCA, LCCA and LSCA, respectively. However, flow rates of oxygenated blood to all other vessels decreased during P4. For example, during P1 and the healthy simulated case, the LCI received 0.55 L/min of oxygenated blood. This value decreased to 0.22 L/min during P4.

These results were supported by their associated mixing zones (Fig. 4). At P1, the mixing zone was located in the abdominal aorta and only a slight advancement of this zone was observed in P2. In P3, the mixing zone reached the descending aorta, while P4 showed blood from VA ECMO being distributed throughout the aorta with high concentrations located at the aortic arch and lower concentrations distal to the arch.

80% VA ECMO Support

With an increased cannula flow rate, P4 was able to provide increased flow from the ECMO circuit to the aortic arch branches (Fig. 3). The BCA, LCCA and LSCA received 0.43, 0.07 and 0.46 L/min of blood from the VA ECMO circuit, respectively. Compared to a healthy adult, these flow rates are 81%, 67% and 109% of normal flow rates usually seen in the BCA, LCCA and LSCA, respectively. The arch vessels did not receive blood from VA ECMO during P1, P2 and P3. Instead, increased perfusion of blood from VA ECMO was seen in all branches below the arch.

Visualizing the distribution of blood from VA ECMO shows a higher concentration of oxygenated blood distributed throughout the aorta during P4 (Fig. 4). At P3, the mixing zone was located at the distal end of the aortic arch. P2 showed slight advancement of the mixing zone within the descending aorta compared to P1. All branches below the arch were completely perfused with blood from the VA ECMO circuit between P1 and P3.

90% VA ECMO Support

During this scenario, P4 showed even greater perfusion of blood from VA ECMO to the arch branches. Compared to a healthy adult, flow to the aortic arch branches from the VA ECMO circuit were 94%, 110% and 109% of normal flow rates usually seen in the BCA, LCCA and LSCA, respectively. The BCA received much greater perfusion of oxygenated blood when compared to other positions: 0.50 L/min at P4, compared to 0.07, 0.09 and 0.11 L/min at P1, P2 and P3 respectively (Fig. 3). Interestingly, total flow (combination of native blood and blood from VA ECMO) to the arch vessels decreased between P3 and P4 (by a total of 0.04 L/min). Due to continuity, this decrease was associated with an increase in total flow to all branches below the arch. For example, total flow to the BCA decreased by 0.03 L/min and total flow to the coeliac axis increased by 0.01 L/min.

The location of the mixing zones for P1, P2 and P3 was in the aortic arch, adjacent to the BCA, with minimal variation for all three positions. Accordingly, blood from the ECMO circuit perfused the LCCA and LSCA for P1, P2, and P3, comparable to native perfusion in a healthy state. For P4, however, homogenous mixing of VA ECMO blood was seen throughout the aorta, beginning in the aortic root.

Afterload Assessment

The effect of cannula advancement on cardiac afterload, is presented in Table 1. Slight increases in systolic and diastolic pressure were observed as the cannula was advanced from P1 to P3. Mean aortic pressures (MAP) also slightly increased with a maximum increase of 6 mmHg during 90% VA ECMO support between P1 and P3. Interestingly, MAP decreased between P3 and P4 during all support cases. As expected, as VA ECMO support increased, a narrowing of pulse pressure was seen, with a decrease in systolic pressure and increase diastolic pressure.

Table 1
Pressure data recorded at the aortic valve for each simulation.

	Systolic/Diastolic Pressures and MAP (mmHg)			
	Position 1	**Position 2**	**Position 3**	**Position 4**
50% VA ECMO Support	103/58, 75	104/59, 76	106/60, 77	106/59, 76
80% VA ECMO Support	86/68, 75	89/71, 77	91/73, 80	90/71, 78
90% VA ECMO Support	80/72, 75	84/75, 78	87/77, 81	84/75, 78
Abbreviations; MAP - mean aortic pressure, VA ECMO - Venoarterial extracorporeal membrane oxygenation				

Discussion

In a simulation setting, we demonstrated that more proximal arterial cannula tip positioning within the aorta improves VA ECMO blood perfusion to the aortic arch branches. This finding was present even during low levels of support when the cannula tip was placed in P4. We also found much higher perfusion of blood from VA ECMO to the brachiocephalic artery (BCA) during P4 at 90% support compared to all other positions, thereby demonstrating the capacity to reduce the incidence of differential hypoxia.

Differential hypoxia is a common and potentially catastrophic complication caused by the competing flow dynamics between native left ventricular ejection and perfusion from the VA ECMO circuit. In a single center study that involved 720 ECMO patients, Rupprecht et al. reported an incidence rate of 8.8% for complications arising due to upper body hypoxia [5]. This was the second most frequent complication they observed and often required intervention to improve upper body oxygen saturation levels. Differential hypoxia is associated with poor perfusion of oxygenated blood to the brain. For example, Pozzebon et al. reported cerebral desaturation (defined as < 60% oxygen saturation for > 5% ECMO duration) in 43 (74%) ECMO patients using near-infrared spectroscopy applied to the patients' foreheads [17]. Moreover, 18 (42%) of these patients went on to develop acute cerebral complications such as stroke and brain death. However, patients with no cerebral de-saturation experienced no acute cerebral complications. Clinical interventions for improving cerebral oxygenation include relocation of the arterial cannula to more proximal locations such as the right subclavian artery and also changing the VA ECMO circuit to a VA-Venous configuration [5, 6, 17–19]. Changing the VA ECMO circuit configuration in this manner is a common method of treating differential hypoxia but involves an additional cannulation site, which can increase the risk of bleeding. It is clear that current clinical practices in peripheral VA ECMO are not systematically structured to prevent differential hypoxia.

Perfusion of blood from VA ECMO to the brachiocephalic artery (BCA) has not been seen in previous simulation studies unless maximum cannula flow rates were used [7, 8, 11]. These studies showed that high cannula flow rates (4 L/min and above) were required to establish a mixing zone in the aortic arch

whilst a cannula flow rate of 5 L/min was required to adequately perfuse the BCA with blood from the VA ECMO circuit. In our study, however, the BCA received oxygenated blood even during lower levels (50%) of support when placed in P4. Additionally, during 90% VA ECMO support and P4, blood from the cannula was homogenously distributed throughout the entirety of the aorta.

Despite not modelling the coronary arteries in this model, blood from VA ECMO appeared to reach the aortic valve during P4 at 90% support. Therefore, perfusion of the coronary vessels was likely achieved during this scenario. In other CFD and in-vitro based studies, the potential for improved coronary perfusion with blood from the ECMO circuit was not observed, even at high ECMO flow rates (> 4.5 L/min) [7–9, 11, 20, 21]. For example, Hoeper et al demonstrated that clinical VA ECMO support with an arterial cannula tip placed within the common iliac artery and a flow rate of 4.5 L/min (similar to P1 during our 90% support case) resulted in a mixing zone in the aortic arch, identified using CT [21]. These results, which agree with those obtained in our simulation study, concluded that despite maximal increases in cannula flow rates (and for typically positioned cannulae), the ascending aorta and coronary arteries do not receive oxygenated blood from the VA ECMO circuit thereby potentially resulting in cardiac hypoxia and inadequate conditions for cardiac recovery. An advanced arterial cannula tip has been attempted clinically as described by Rodriguez and Maharajh who implemented this technique in two pediatric patients [12]. In their study, a 19 Fr drainage cannula was used in an off-label manner in place of an arterial cannula because there are no commercially available arterial cannulae capable of proximal positioning. The cannula tip was advanced until the tip lay distal to the left subclavian artery (similar to P4 in our study) and a flow rate of 83 ml/kg/min was used. Both patients showed no signs of differential hypoxia during ECMO support and showed improved hemodynamics and saturations.

An important implication of our results is the use of P4 in cases of ECPR where maximizing cerebral perfusion is a priority [22]. Despite the high cannula blood flow rate during 90% support (4.5 L/min), in P1 only 12% of the flow to the BCA consisted of blood from VA ECMO. This is concerning as P1 reflects the most common arterial tip position used in current clinical practice [3]. Instead, our results demonstrated much higher cerebral perfusion of oxygenated blood to the BCA is possible at P4 with the added benefit of possible coronary perfusion at 90% support. This is particularly important in cardiogenic shock after acute myocardial infarction and in the setting of ischemic heart disease. Therefore, cannula tip position may be an important factor in preventing not only neurological injury in patients treated with ECPR but also cardiac injury.

While placement of the cannula in P4 resulted in increased oxygenated VA ECMO perfusion of the aortic arch vessels in our study, there was a decrease in the proportion of VA ECMO blood reaching all other vessels. In particular, VA ECMO perfusion of the two common iliac vessels decreased by more than half with P4 compared to P1 during 50% VA ECMO support. This is supported by numerical results from Bongert et al. who showed that advancing the cannula tip from the femoral artery to the abdominal aorta resulted in lower perfusion of blood from VA ECMO to the lower limbs [23].

We also found advancing the cannula caused a minor increase in afterload compared to other cannula positions. Only a maximum increase of 6 mmHg was observed in P3 compared to P1. However, a slight decrease in MAP between P3 and P4 was found for all levels of support. This can be attributed to an increase in total flow to the lower branches (from LV and VA ECMO) and a decrease in total flow to the arch branches in P3.

An increase in arterial cannula insertion length may cause concern due to increased cannula resistance. However, the maximum pressure-drop observed was 160 mmHg (P4 at 90% support). This pressure-drop can be achieved by clinically used VA ECMO pumps by increasing pump speed accordingly as usually done when using arterial cannulas of smaller diameter [24]. For example, Stephens et al. demonstrated that a 15 Fr arterial cannula was able to provide targeted full ECMO support with a pressure drop of 282 mmHg across the cannula [25].

Various studies have previously investigated mixing zone location during VA ECMO using a CFD model [7–11]. However, these studies primarily involved variation of VA ECMO flow rates with a constant cannula position throughout. Cannulas were placed more distal to P1 from our study but tip placement was still within a common iliac artery. Comparison of results between our study (during P1) and Stevens et al. show good agreement at 50% support [8]. However, their exclusion of major vessels such as the SMA and IMA result in a much higher mixing zone location at 80% support. Nezami et al. used an idealized geometry which contained all the major vessels used in our study, and showed good agreement with respect to mixing zone locations and vessel perfusion at al support levels when our cannula was placed in P1 [7]. In both aforementioned papers, however, cannula length was excluded from their models and was addressed as a limitation.

Limitations

We assumed the aortic walls to be rigid in our simulations. Incorporating wall deformability would require much higher computational power than was feasible for the number of simulations conducted. However, Nezami et al. included wall deformability and their mixing zone results showed negligible difference to simulations conducted with rigid vessel walls [9]. Secondly, the resistance and compliance parameters used in the Windkessel model reflect healthy patient conditions. Thus, any differences in these parameters associated with the heart failure state or vasopressor drugs were not simulated. Additionally, cardiac chamber pressure volume relations and autonomic nervous system autoregulatory mechanisms such as the baroreflex were not modelled in this study. Thus, cardiac and vascular changes in response to VA ECMO implementation were not simulated. Lastly, the results produced in this study have not been validated using in-vivo or in-vitro data. Therefore, all results should be interpreted with caution until experimental or clinical validation is performed.

Conclusion

In a simulation study, advancing the arterial cannula tip further into the aorta provides increased perfusion of oxygenated blood from the VA ECMO circuit to the aortic arch vessels at all levels of VA ECMO support. If translated to the clinical setting, this approach may reduce the incidence of differential and/or cerebral hypoxia. In comparison, standard arterial cannula tip position was predicted to result in differential hypoxia at both 50% and 80% support with only a moderate improvement at 90% support. These findings can inform clinicians in their choice of cannula length and position, and can form the basis of new cannula design.

Abbreviations

VA ECMO – Venoarterial Extracorporeal Membrane Oxygenation

CFD – Computational Fluid Dynamics

P1, P2, P3 and P4 – Position 1, Position 2, Position 3 and Position 4

CT – Computed Tomography

ECPR – Extracorporeal Cardiopulmonary Resuscitation

BCA – Brachiocephalic Artery

LCCA – Left Common Carotid Artery

LSCA – Left Subclavian Artery

SMA – Superior Mesenteric Artery

IMA – Inferior Mesenteric Artery

LCI – Left Common Iliac

RCI – Right Common Iliac

LV – Left Ventricle

MAP – Mean Aortic Pressure

Declarations

Ethics Approval and Consent to Participate

Anonymized patient imaging and demographic data was used in this article in accordance with ethics approval from The Alfred Ethics Committee. Therefore, informed consent was not required.

Consent for Publication

This manuscript has been approved for publication for this journal by all authors. Informed consent was not required from the patient as their imaging and demographic data was used in accordance with ethics approval from The Alfred Ethics Committee.

Availability of Data and Materials

All data generated or analyzed during this study are included in this published article and its supplementary information files.

Competing Interests

The authors declare that they have no competing interests

Funding

This work was supported by Monash University. Shaun D Gregory is the recipient of a Fellowship (102062) from the National Heart Foundation of Australia.

Authors' Contributions

JR and RB proposed the idea of a long arterial cannula that could be positioned close to the arch of the aorta to maximize blood flow to the brain during ECMO; this was based on preliminary unpublished animal work. AW designed the study, developed the CFD model, conducted the CFD simulations and wrote the main draft of the manuscript. AB and MS designed the study and provided valuable clinical input towards the final draft of the manuscript. AS, MS, AV and MK aided in the interpretation of the data and provided vital contributions to the drafting of the manuscript. AV and MK also provided assistance with CFD modelling. JR and RB provided valuable clinical input and contributed towards the final draft of the manuscript contents. SG designed the study, aided in the interpretation of data and contributed towards the final draft of the manuscript.

Acknowledgements

The authors wish to acknowledge Dr. Tim Joseph for their efforts in acquiring the computed tomography scans which were then used to generate the 3D model of the aorta.

References

1. Pavlushkov E, Berman M, Valchanov K. Cannulation techniques for extracorporeal life support. Annals of translational medicine 2017;5(4).
2. Strunina S, Hozman J, Ostadal P. The peripheral cannulas in extracorporeal life support. Biomedical Engineering/Biomedizinische Technik 2019;64(2):127–33.
3. Jayaraman AL, Cormican D, Shah P, Ramakrishna H. Cannulation strategies in adult veno-arterial and veno-venous extracorporeal membrane oxygenation: techniques, limitations, and special considerations. Annals of cardiac anaesthesia 2017;20(Suppl 1):S11.
4. Lorusso R, Barili F, Mauro MD, Gelsomino S, Parise O, Rycus PT, et al. In-hospital neurologic complications in adult patients undergoing venoarterial extracorporeal membrane oxygenation: results from the extracorporeal life support organization registry. Critical care medicine 2016;44(10):e964-e72.
5. Rupprecht L, Lunz D, Philipp A, Lubnow M, Schmid C. Pitfalls in percutaneous ECMO cannulation. Heart, lung and vessels 2015;7(4):320.
6. Contento C, Battisti A, Agrò B, De Marco M, Iaiza A, Pietraforte L, et al. A novel veno-arteriovenous extracorporeal membrane oxygenation with double pump for the treatment of Harlequin syndrome. Perfusion 2020;35(1_suppl):65–72.
7. Nezami FR, Khodaee F, Edelman ER, Keller SP. A computational fluid dynamics study of the extracorporeal membrane oxygenation-failing heart circulation. ASAIO Journal 2021;67(3):276–83.
8. Stevens M, Callaghan F, Forrest P, Bannon P, Grieve S. Flow mixing during peripheral veno-arterial extra corporeal membrane oxygenation–a simulation study. Journal of biomechanics 2017;55:64–70.
9. Nezami FR, Ramezanpour M, Khodaee F, Goffer E, Edelman ER, Keller SP. Simulation of Fluid-Structure Interaction in Extracorporeal Membrane Oxygenation Circulatory Support Systems. Journal of Cardiovascular Translational Research 2021:1–9.
10. Zhang Q, Gao B, Chang Y. The numerical study on the effects of cardiac function on the aortic oxygen distribution. Medical & biological engineering & computing 2018;56(7):1305–13.
11. Prisco AR, Aguado-Sierra J, Butakoff C, Vazquez M, Houzeaux G, Eguzkitza B, et al. Concomitant Respiratory Failure Can Impair Myocardial Oxygenation in Patients with Acute Cardiogenic Shock Supported by VA-ECMO. Journal of cardiovascular translational research 2021:1–10.
12. Rodriguez ML, Maharajh G. Long venous cannula on the arterial position for VA-ECMO. Perfusion 2018;33(6):423–5.
13. Xiao N, Alastruey J, Alberto Figueroa C. A systematic comparison between 1-D and 3-D hemodynamics in compliant arterial models. International journal for numerical methods in biomedical engineering 2014;30(2):204–31.
14. Alastruey J, Xiao N, Fok H, Schaeffter T, Figueroa CA. On the impact of modelling assumptions in multi-scale, subject-specific models of aortic haemodynamics. Journal of The Royal Society Interface 2016;13(119):20160073.

15. Cho YI, Kensey KR. Effects of the non-Newtonian viscosity of blood on flows in a diseased arterial vessel. Part 1: Steady flows. Biorheology 1991;28(3–4):241–62.
16. Caballero A, Laín S. Numerical simulation of non-Newtonian blood flow dynamics in human thoracic aorta. Computer methods in biomechanics and biomedical engineering 2015;18(11):1200–16.
17. Pozzebon S, Blandino Ortiz A, Franchi F, Cristallini S, Belliato M, Lheureux O, et al. Cerebral near-infrared spectroscopy in adult patients undergoing veno-arterial extracorporeal membrane oxygenation. Neurocritical care 2018;29(1):94–104.
18. Wilson J, Fisher R, Caetano F, Soliman-Aboumarie H, Patel B, Ledot S, et al. Managing Harlequin Syndrome in VA-ECMO–do not forget the right ventricle. Perfusion 2021:02676591211020895.
19. Honore PM, Gutierrez LB, Kugener L, Redant S, Attou R, Gallerani A, et al. Risk of harlequin syndrome during bi-femoral peripheral VA-ECMO: should we pay more attention to the watershed or try to change the venous cannulation site? Critical Care 2020;24(1):1–3.
20. Kato J, Seo T, Ando H, Takagi H, Ito T. Coronary arterial perfusion during venoarterial extracorporeal membrane oxygenation. The Journal of thoracic and cardiovascular surgery 1996;111(3):630–6.
21. Hoeper MM, Tudorache I, Kühn C, Marsch G, Hartung D, Wiesner O, et al. Extracorporeal membrane oxygenation watershed. Circulation 2014;130(10):864–5.
22. Sakamoto T, Morimura N, Nagao K, Asai Y, Yokota H, Nara S, et al. Extracorporeal cardiopulmonary resuscitation versus conventional cardiopulmonary resuscitation in adults with out-of-hospital cardiac arrest: a prospective observational study. Resuscitation 2014;85(6):762–8.
23. Bongert M, Gehron J, Geller M, Böning A, Grieshaber P. Cannula position and Bernoulli effect contribute to leg malperfusion during extracorporeal life support with femoral arterial cannulation—an in silico simulation study. Interactive cardiovascular and thoracic surgery 2019;29(2):312–9.
24. Lehle K, Philipp A, Müller T, Schettler F, Bein T, Schmid C, et al. Flow dynamics of different adult ECMO systems: a clinical evaluation. Artificial organs 2014;38(5):391–8.
25. Stephens AF, Wickramarachchi A, Burrell AJ, Bellomo R, Raman J, Gregory SD. The Hemodynamics of Small Arterial Return Cannulae for Venoarterial Extracorporeal Membrane Oxygenation. Artificial Organs 2022.

Figures

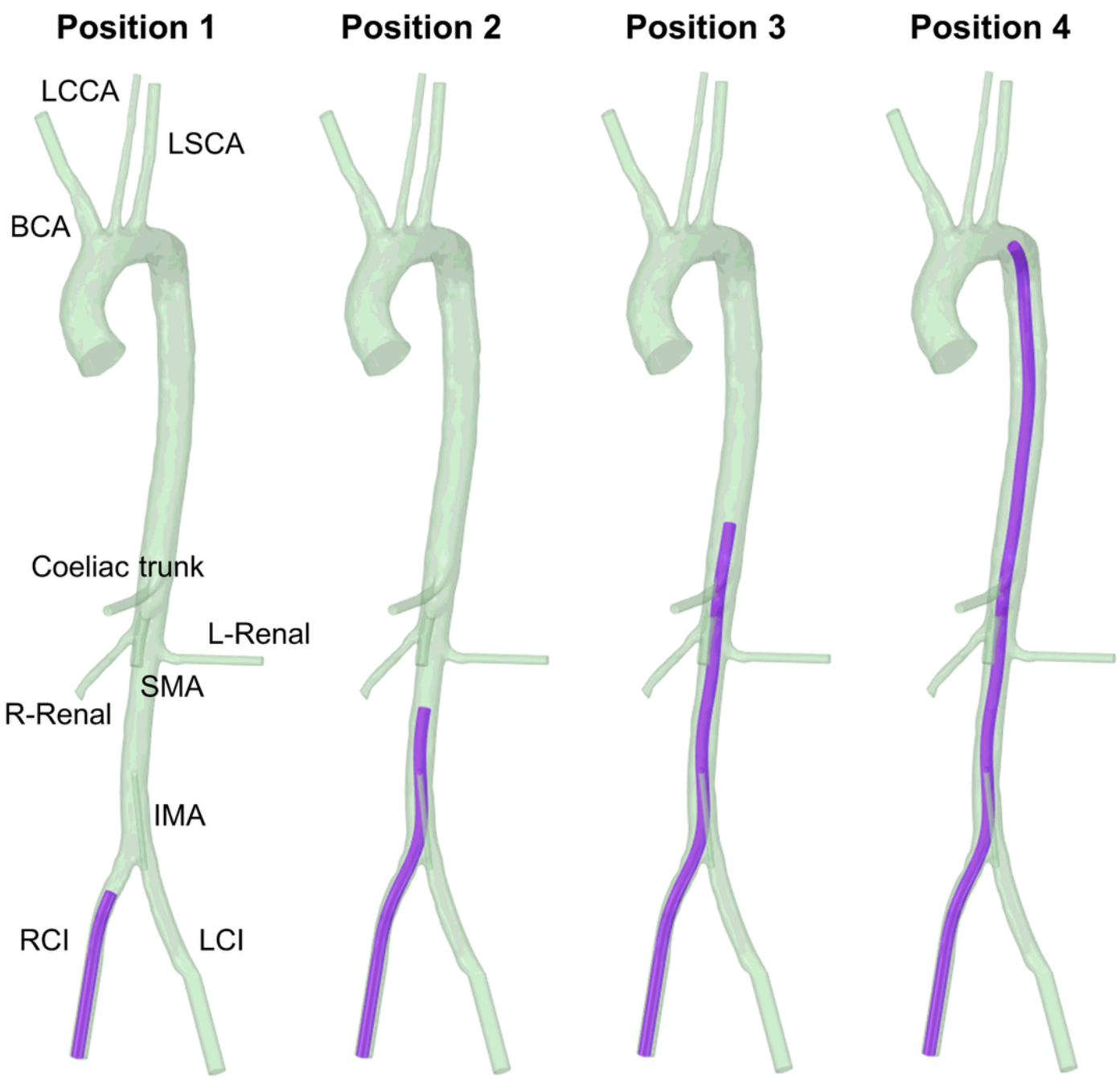

Figure 1

Cannula tip positions investigated. Position 1, in the right iliac artery; Position 2, in the abdominal aorta; Position 3, in the descending aorta; and Position 4, in the aortic arch. BCA – brachiocephalic artery, LCCA – left common carotid artery, LSCA – left subclavian artery, L-Renal – left renal, R-Renal – right renal, SMA – superior mesenteric artery, IMA – inferior mesenteric artery, RCI – right common iliac, LCI – left common iliac.

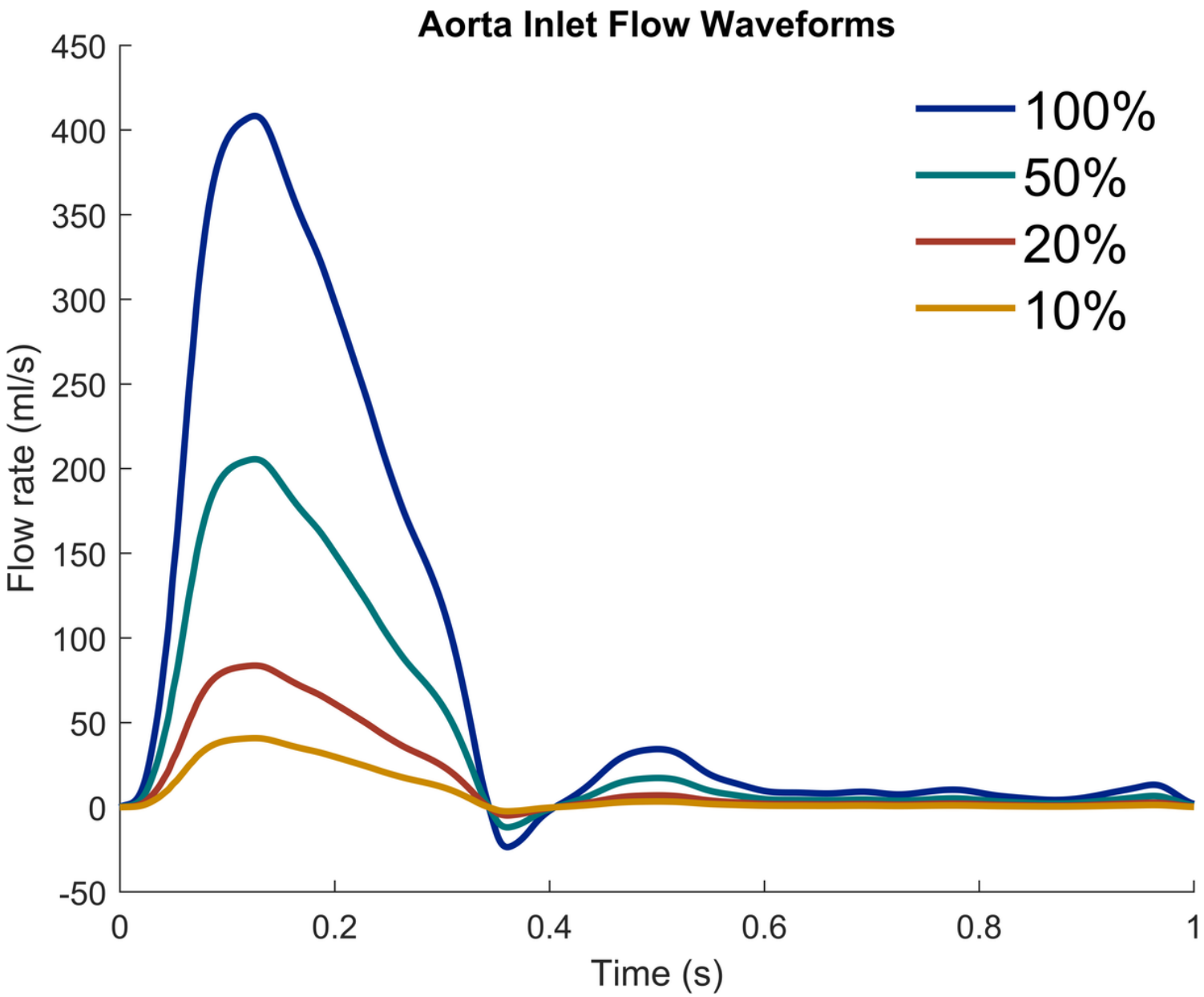

Figure 2

Scaled aortic valve inlet profiles to reflect different severities of cardiac dysfunction. Here, 100% reflects healthy cardiac function where 5 L/min of cardiac output from the left ventricle. 50%, 20% and 10% depicts cardiac failure where only 2.5, 1 and 0.5 L/min of cardiac output from the left ventricle, respectively.

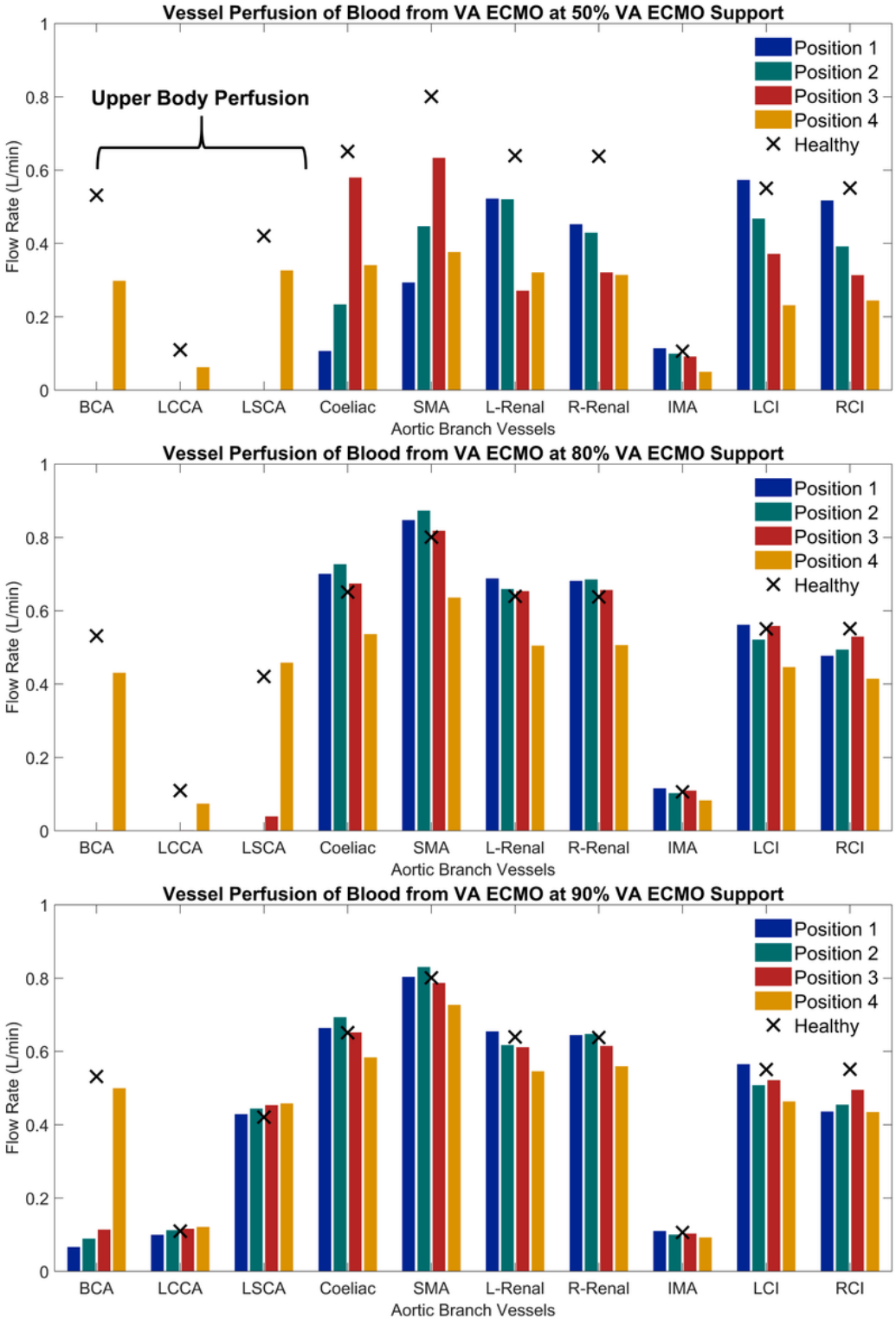

Figure 3

Vessel perfusion rates from VA ECMO, with varying cannula tip position and 50%, 80% and 90% ECMO support. BCA – Brachiocephalic artery, LCCA – Left Common Carotid artery, LSCA – Left Subclavian artery, SMA – Superior Mesenteric artery, L-Renal – Left Renal artery, R-Renal – Right Renal artery, IMA – Inferior Mesenteric artery, LCI – Left Common Iliac artery and RCI – Right Common Iliac artery

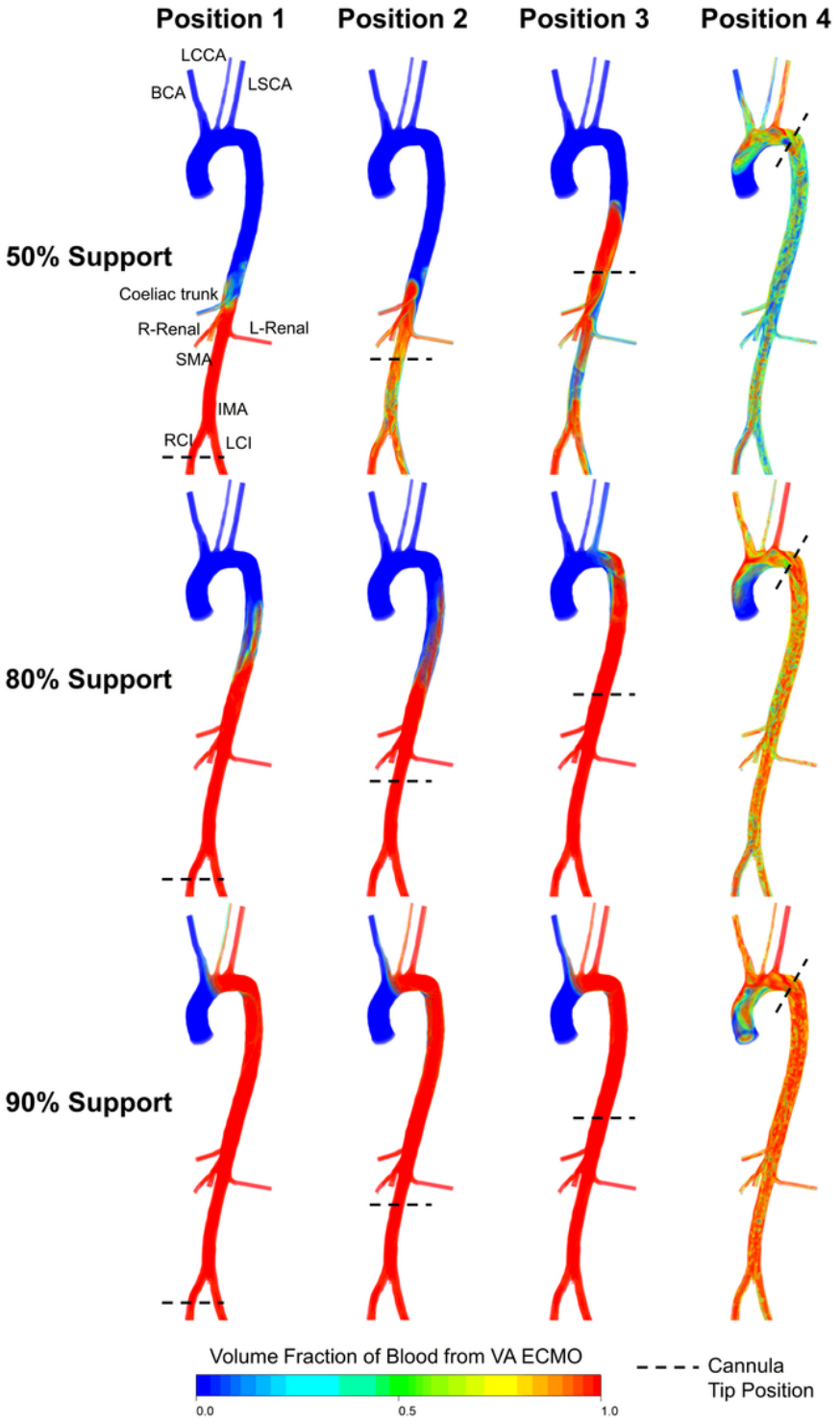

Figure 4

VA ECMO blood distribution represented as volume fractions for each support level and cannula position. In this figure, the red color (volume fraction of 1) refers to oxygenated blood provided by the circuit, whereas blue refers to blood from the LV, and hence, an absence of oxygenated blood (volume fraction of 0). BCA – brachiocephalic artery, LCCA – left common carotid artery, LSCA – left subclavian artery, L-

Renal – left renal, R-Renal – right renal, SMA – superior mesenteric artery, IMA – inferior mesenteric artery, RCI – right common iliac, LCI – left common iliac.

Supplementary Files

This is a list of supplementary files associated with this preprint. Click to download.

- GraphicalAbstract.png
- AdditionalFile1.docx
- AdditionalFile2.docx